

【論文】

Proposal for Hybrid Stress-Ribbon Vehicle Bridges

Part 1. Preliminary design of superstructure and static characteristics

Takehiko Harada[†], Takeshi Yoshimura[†], Yoji Mizuta[†], Takahisa Tanaka[†],
Takuma Beppu[‡], Hideo Jo[‡], Niels J. Gimsing^{**} and Won-Ho Kang^{***}

ハイブリッド吊床版道路橋の提案 (その1) 上部工の試設計と静力学特性

原田 健彦[†], 吉村 健[†], 水田 洋司[†], 田中 孝久[†], 別府 琢磨[‡],
城 秀夫[‡], N. J. ギムスィング^{**}, 姜 圓鎬^{***}

Abstract: In our previous study, a design concept for hybrid stress-ribbon pedestrian bridges was proposed. In this paper, hybrid stress-ribbon vehicle bridges with a span length of $L=200, 400$ or 600 m are proposed, and the preliminary design of superstructure and the examination of their static characteristics are made. The findings revealed that the weight of the stiffening truss girder per unit area was about half of a streamlined steel box girder for a conventional suspension bridge, and that the total number of the upper and lower cable strands was respectively found to be 16, 40 and 60. The diameters of the 16-, 40- and 60-strand single cable were estimated to be 26, 40 and 50 cm and were not too large. Regarding the static characteristics, the deformation and deflection of girder were well controlled by the upper cable, and the maximum normal force in the lower cable was 90% of the resisting force. Therefore, the above results suggest that the design concept for the proposed hybrid stress-ribbon structure could be applied to vehicle bridges with a single span of 200-600 m.

Keywords: hybrid stress-ribbon vehicle bridge; suspension bridge; preliminary design; static characteristics.

1. Introduction

In deep and wide V-shaped valleys, fjords or lias coasts, engineers often face difficulties in building bridge foundations. In view of this, the authors proposed a type of hybrid bridge based on the stress-ribbon concept as a collaboration of professors and bridge engineers between Japan and Korea as well as Denmark. Stress-ribbon is considered to be one of the practical applications for crossing these wide and deep spaces because the bridge has a single span without any pier. Also, the ground of these locations consists of hard rock, and therefore, the ground-anchored abutments and the ground-anchored anchorages must be constructed economically.

In our earlier study, hybrid steel stress-ribbon 'pedestrian' bridges with a single span length of 123 m were proposed. The preliminary design and their static and the aerodynamic characteristics as well as seismic response were examined¹⁻³⁾. These bridges were designed

as alternative structures of an existing conventional concrete stress-ribbon bridge.

This paper is the full-length paper in the Proceedings of 3rd Int. Conf. on Advances in Structural Eng. and Mech.⁴⁾, and is composed of two parts. In part 1, a proposal is made for hybrid stress-ribbon 'vehicle' bridges with a single span length of $L=200, 400$ or 600 m. These bridges were preliminarily designed and their static characteristics were examined. In part 2⁵⁾ of this study, the details of the results obtained in a numerical analysis in the cable design are reported.

The objective of this paper is to verify whether or not the design concept for the hybrid stress-ribbon structure can be applied to single span vehicle bridges with $L=200-600$ m.

2. Hybrid stress-ribbon pedestrian bridge

At the earlier stage of this study, a hybrid stress-ribbon pedestrian bridge was proposed¹⁾. This bridge was an alternative structure of an existing conventional prestressed concrete stress-ribbon pedestrian bridge, the Jinyanomori Bridge in Oita Prefecture, Japan. To decrease the extremely large tensile force in the inner cables of the concrete bridge, a hybrid

[†] Dept. of Civil & Urban Design Eng., Kyushu Sangyo Univ.

[‡] Yokogawa Construction Co., Ltd.

^{**} Fukuoka Branch, Structural Engineering Center Co., Ltd.

^{**} Dept. of Civil Eng., Technical Univ. of Denmark

^{***} Division of Construction, Collage of Eng., Dong-A Univ.

structure of stress-ribbon and suspension bridge, which is referred to as 'a stress-ribbon suspension bridge', of light steel construction was proposed. In this proposal, more than 50% of the 'lower' (inner) cables were stretched outside, over the deck. These 'upper' cables were supported by newly installed concrete towers and suspended the deck with vertical suspenders. In order to increase its aerodynamic stability, an open grating deck plate, a pair of circular edge beams as well as a quasi-closed cross-section were used in this bridge.

The findings in the earlier study revealed that the weight of the bridge girder and the horizontal component of tensile force in the cables was 1/12 and 1/6 of the conventional concrete structure, respectively, and that the critical flutter speed both during erection of the girder and after completion was sufficiently high.

3. Conditions of location

It is very important that hybrid stress-ribbon vehicle bridges must be competitive in design competition in the cases where the bridge construction site is located in a wide and very deep V-shaped valley, fjord or lias coast. The reason for this is that on these sites, bridge engineers often have to deal with difficulties in building foundations, especially with the construction of pylons and piers that are not necessary for the hybrid structures. Since the ground of these locations consists of hard rock, the ground-anchored abutments and ground-anchored anchorages are available, so these substructures must be constructed economically. In these hybrid structures, not only the upper cables but also the lower cables must be sufficiently effective for the erection of the girder.

4. Proposal for hybrid stress-ribbon vehicle bridges

4.1. Outline of proposal

Fig. 1 shows a concrete cable-stayed bridge, the Ayunose Bridge, recently completed in Kumamoto Prefecture, Japan. The bridge has a total length of about

400 m for a '140 m deep V-shaped valley' crossing. The deep valley with steep natural slopes of the area posed difficulties for engineers in building the pylon and the pier.

Fig. 2(a) presents our proposal for a hybrid stress-ribbon bridge as an alternative design of this cable-stayed bridge. The bridge has a single span of $L=400$ m. The effective width of the girder is 10.5 m with two traffic lanes and one sidewalk (Fig. 2(b)). As shown in Figs. 2(a) and (c), the superstructure of this proposed bridge consists of the reinforced concrete towers, the upper and backstay cables supported by the towers, the lower cables stayed by the ground-anchored abutments and the girder. The 13 m wide steel girder is composed of a pair of edge beams of circular pipe with a diameter of 70 cm, the open-grating deck plate, the I-shaped floor beams with varying depth of 0.7-2 m, the upper lateral bracings and the lower inclined bracings. The sag ratios (f/L) of the upper cable and lower cable are 0.1 and 0.02, respectively, which are the same values as those applied to the hybrid stress-ribbon pedestrian bridge¹⁾.

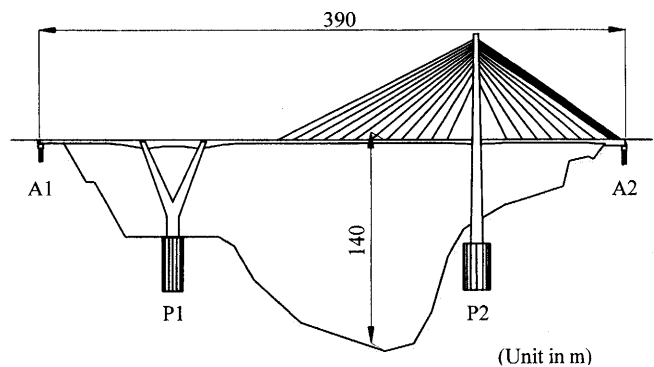


Fig. 1 The Ayunose Bridge, a concrete cable-stayed vehicle bridge.

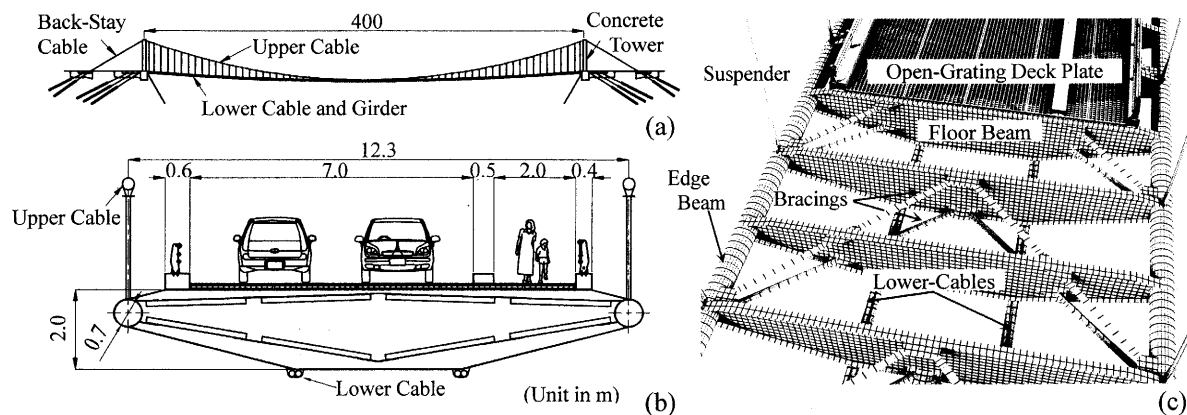


Fig. 2 The side view, (a), and the cross-section and CG of the girder, (b) and (c), for the hybrid stress-ribbon vehicle bridge.

4.2. Characteristics of structure

The edge beam is fixed to the ground anchored abutments in order that the axial tensile force under live load is induced in the beam to partially function as the ‘stress-ribbon’. In this proposed structure, the edge beam and the lower cable also function as the upper chord and the lower chord of the ‘stiffening truss girder’, respectively*1.

The upper lateral bracings and the lower inclined bracings form a quasi-closed cross-section in order to increase the torsional stiffness of the girder. The quasi-closed cross-sectional area enclosed by the bracings can be increased by an increase in the depth of the floor beams in cases where much higher torsional stiffness is required. It has already been shown that the aerodynamic stability of the hybrid structure is greatly increased by means of the quasi-closed cross-section, the open grating deck as well as the circular edge beams¹⁾.

The preliminary design and the examination of static characteristics were made not only for the proposal of the bridge with $L=400$ m but also for the other proposal of two bridges with $L=200$ and 600 m. In these bridges, it is assumed that the dimensions of the girder, the sag ratios of the cables, the material of the superstructure are the same.

5. Preliminary design

5.1. Open grating deck

The 6 m long, 2 m wide and 15 cm deep standard steel open grating deck plates were available (Fig. 3). This 6 m long deck plate was originally designed as a two-span two-dimensional continuous beam for A-live load specified in the specifications for Japan highway

bridges shown below. Therefore, each floor beam that supports the deck plate should be placed with the space of 3 m. It is expected that the deck may function as an orthotropic steel plate deck in cases where the deck plate can be fixed firmly to the upper flange plate of the floor beam. In order to make an innovation in fabricating this ‘quasi-orthotropic steel deck’, the following further studies are necessary: developing a method of connecting the deck plate to the upper flange of floor beam as well as solving the problem of buckling of the deck plate under compressible force introduced by the bending moment in the ‘stiffening truss’.

5.2. Floor beam

Although the 12.3 m long welded steel floor beam is a three-span continuous beam elastically supported by a pair of upper cables on both sides and a pair of lower cables at the mid-span, the floor beam was assumed to be a simply supported beam with a span length of 12.3 m

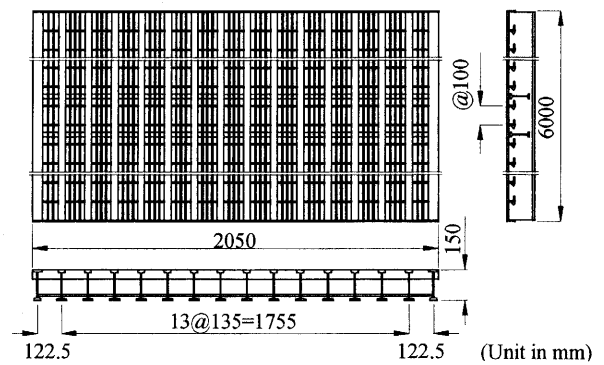
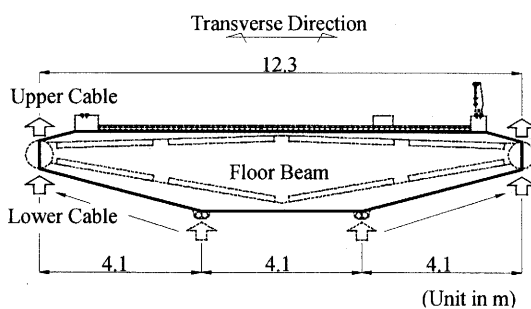
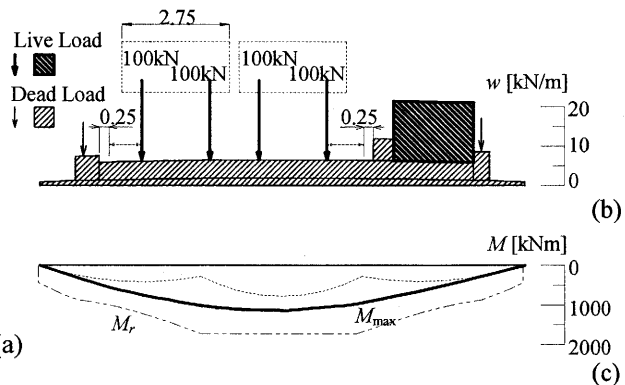


Fig. 3 The standard open grating steel deck plate.



(a)



(b)

(c)

Fig. 4 The floor beam assumed to be a simply supported beam by the upper and lower cables, (a), A-live load and dead load acting on the floor beam, (b), and the maximum bending moment diagram and resisting moment diagram, (c).

*1 In order that the compressive force due to live load may not be induced in the lower cable, the pretension force due to dead load of the girder together with the cable weight was introduced in the lower cable (section 6.1).

*2 Two pairs of concentrated traffic load of 100 kN and distributed footway track live load of 5 kN/m² were taken into account in the design specified in the specification of Japan highway bridges.

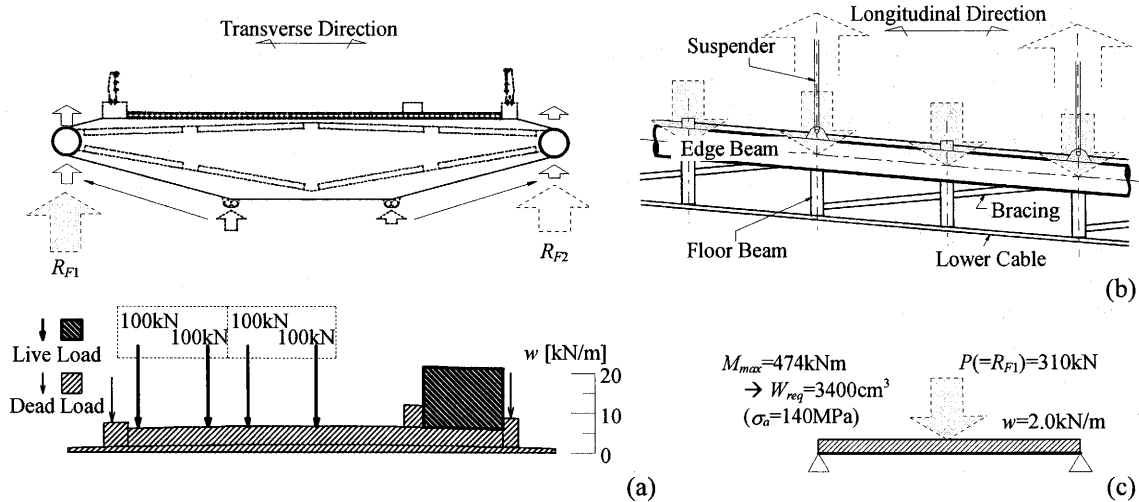
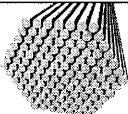


Fig. 5 A-live load and dead load acting on the mid floor beam, (a), and the edge beam of 6 m long one segment assumed to be a simply supported beam, (b) and (c).

Table 1 The dimension of parallel-wire strand, PWS-127.

Number of wire	Shape and size [mm]	Cross-sectional area [mm ²]	Guaranteed minimum tensile strength [kN]	Weight [N/m]
127-φ5mm	 57x65	2490	4400	192

for the sake of simplicity in the analysis (Fig. 4(a)). The dead load and A-live load are shown in Fig. 4(b)². The thick solid line in Fig. 4(c) represents the maximum bending moment (M_{\max}) diagram for the floor beam under these dead and A-live loads. Since M_{\max} was far below the resisting moment (M_r) denoted by a chained line in Fig. 4(c), the depth of the floor beam could be below 2 m. However, the depth of 2 m was necessary for an increase in the quasi-closed cross-sectional area enclosed by the upper lateral bracings and lower inclined bracings in the stiffening truss to maintain sufficient high torsional stiffness.

The dotted line in Fig. 4(c) shows the outline of M_{\max} diagram for the elastically supported three-span continuous floor beam under dead and A-live loads. M_{\max} in the figure was much smaller than the one in the simply supported floor beam.

5.3. Edge beam

The edge beam was a rolled shape steel circular pipe with a diameter of 70 cm. One segment of the stiffening truss girder was 6 m long and was supported by vertical suspenders on both sides (Fig. 5(b)). The 6 m long edge beam per one segment was assumed to be a simply supported beam. The maximum bending moment of the edge beam was estimated to be 480 kNm. This maximum bending moment was mainly induced by a 310

kN concentrated load at the span center (Figs. 5(b) and (c)) where the mid floor beam was fixed. The required thickness of the edge beam was estimated to be 12 mm in cases where STK400 (SS400) steel material was used. The stress analysis of the edge beam due to combined bending moment and normal force is discussed in section 6.1.

The total weight of the stiffening truss girder per one segment was estimated to be 200 kN and the weight of the girder per unit deck area was 3.5 kN/m². The weight of 3.5 kN/m² is, for example, about half of the weight of the steel streamlined box girder for the Toyoshima Bridge. This bridge is a $L=540$ m single span suspension bridge with two traffic lanes and one sidewalk under construction in Hiroshima Prefecture, Japan.

As mentioned above, the same preliminary designed girder was applied to three kinds of proposed bridge with $L=200, 400$ and 600 m.

5.4. Upper and lower cables

The details of preliminary design of the upper and lower cables are reported in 'Part 2' of this study⁵. The outline of design and the main results obtained in a numerical analysis are summarized in this section.

The parallel-wire strands, PWS-127, were used for the upper and lower cables. The dimension of the strand

Table 2 The results of strand analysis for three bridges.

L [m]	$N_U + N_L$	N_U	N_L	w_{GU}/w_G	w_{GL}/w_G	w_C [kN/m/Br]
200	16	8	8	0.7	0.3	6.14
400	40	20	20	0.75	0.25	15.4
600	60	30	30	0.85	0.15	23.0

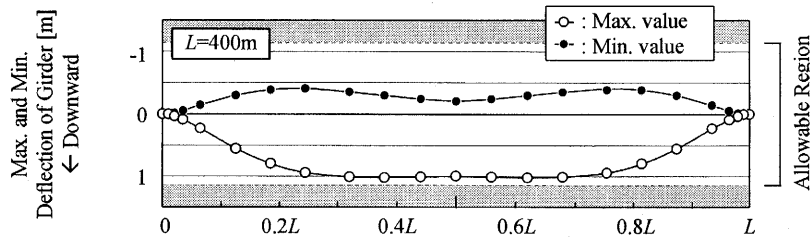


Fig. 6 The maximum and minimum deflection of girder for the bridge with $L=400$ m'.

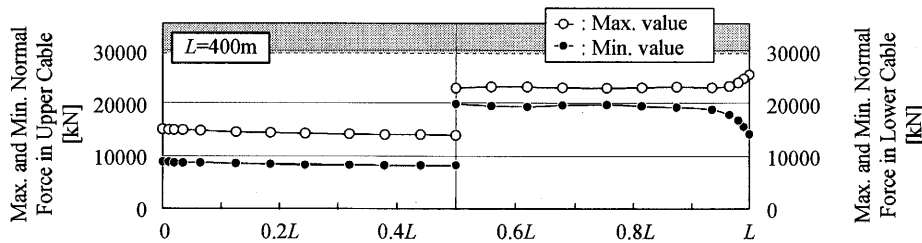


Fig. 7 The maximum and minimum normal force in the upper and lower cables for the bridge with $L=400$ m'.

is listed in Table 1. The optimum required number of the upper and lower cable strands was determined in the preliminary design by a 2D numerical analysis. In the analysis, the optimum number of cable strands was determined in the following manners: the maximum deflection of the girder was below the allowable value of $L/350$, and the maximum normal stress in the upper and lower cables was below the allowable value of 590 MPa under dead load and A-live load. Note that both the upper and lower cables were subjected to uniform load due to dead load of girder, w_{GU} and w_{GL} , and that the initial tensile force in the upper and lower cables was induced by w_{GU} and w_{GL} respectively together with the weight of each cable.

The deflection of the girder and the normal force in the upper and lower cables can be controlled by the following three parameters: (1) the number of upper cable strand per cable, N_U ; (2) the number of lower cable strand per cable, N_L ; (3) the ratio of uniform dead load subjected to the lower (upper) cable in the entire span to dead load of girder, w_{GL}/w_G (w_{GU}/w_G).

The results obtained by a numerical analysis for three bridges are summarized in Table 2. The findings revealed that for the bridges with the span length of 200, 400 and 600 m, the optimum total number of strands, N_U+N_L , was respectively found to be 16, 40 and 60. The diameters of 16-, 40- and 60-strand single cable were estimated to be 26, 40 and 50 cm and were not too large.

6. Static characteristics

6.1. Bridge with $L=400$ m

6.1.1. Deflection of girder

Fig. 6 presents the maximum (downward) and minimum (upward) deflection diagram of girder. In this figure, the non-shadowed area represents the allowable region. The maximum deflection of about 90% of the allowable value, which was considered to be the 'criterion' in the analysis, was observed in a relatively wide range of $L/4 - 3L/4$, while the minimum deflection was far below the allowable value in the entire span.

6.1.2. Normal force in upper and lower cables

Fig. 7 illustrates the maximum and minimum normal force diagram in both the upper and the lower cables. The maximum normal force in the lower cable of about 90% of the resisting force, which was considered to be the 'criterion' in the analysis, was observed not in a wide range of the span but only at the abutment. While, the maximum normal force in the upper cable was far below the resisting force. As described in 'Part 2' of this study⁵⁾, much larger number of upper cable strand (N_U) was required for controlling the deflection of girder than the number for controlling the upper cable stress. It should be noted that the minimum normal force in the cables was verified not to be negative but to be positive; i.e., that the compressive axial force was not induced in the cables.

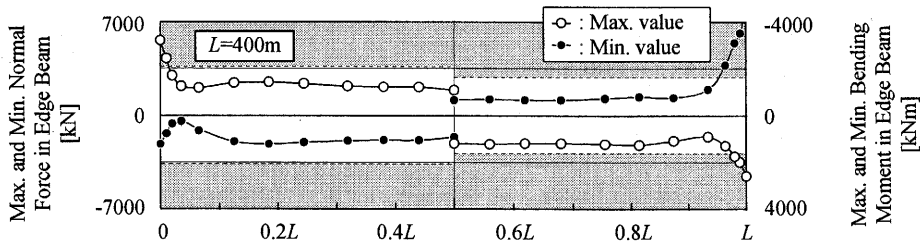


Fig. 8 The maximum and minimum normal force and bending moment in the edge beam for the bridge with $L=400\text{ m}$.

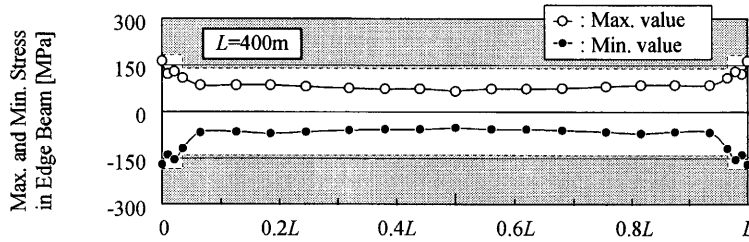


Fig. 9 The maximum and minimum extreme fiber stress due to combined normal force and bending moment for the bridge with $L=400\text{ m}$.

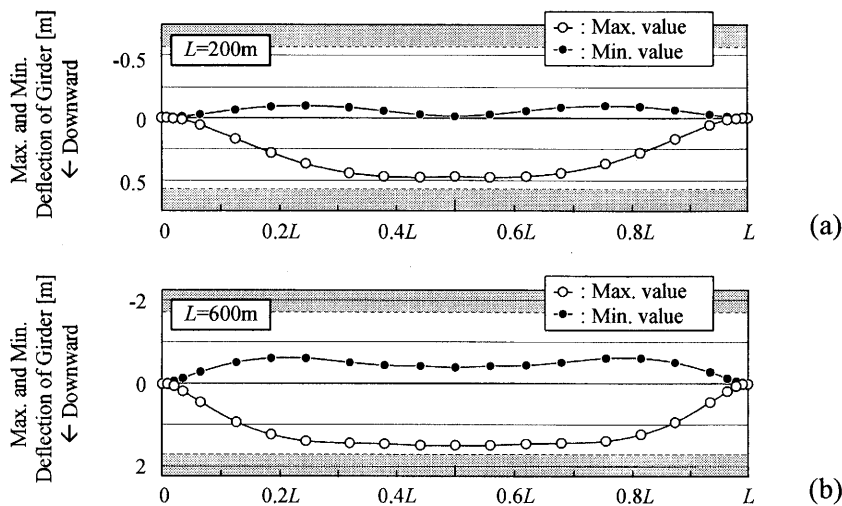


Fig. 10 The maximum and minimum deflection of girder for the bridges with $L=200\text{ m}$ and 600 m , (a) and (b).

6.1.3. Stress due to combined bending moment and normal force in edge beam

As mentioned earlier, the edge beam functions not only as the bending member but also as the normal force member. Therefore, combined bending moment and normal force were induced to the edge beam. Fig. 8 shows the maximum and minimum normal force diagram together with the maximum and minimum bending moment diagram. It is observed that both bending moment and normal force were below the resisting values in the entire span except for the portion close to the abutment.

Fig. 9 shows the maximum and minimum extreme fiber stress diagram of combined bending moment and normal force in the edge beam. Also, the maximum and minimum values were far below the allowable stress of

140 MPa in the entire span except for the portion close to the abutment. This locally over-stressed problem was easily solved by partially using the rolled shape circular pipe with higher allowable stress of 185 MPa (STK490).

6.2. Bridge with $L=200$ or 600 m

Figs. 10(a) and (b) show the maximum (downward) and minimum (upward) deflection diagram of girder for the other two bridges with $L=200$ and 600 m , respectively. Qualitatively, a nominal difference can be seen between these figures and Fig. 6 for the bridge with $L=400\text{ m}$.

Figs. 11(a) and (b) illustrates the maximum and minimum normal force diagram in both the upper and the lower cables for the other two bridges with $L=200$ and 600 m , respectively. Qualitatively, a nominal

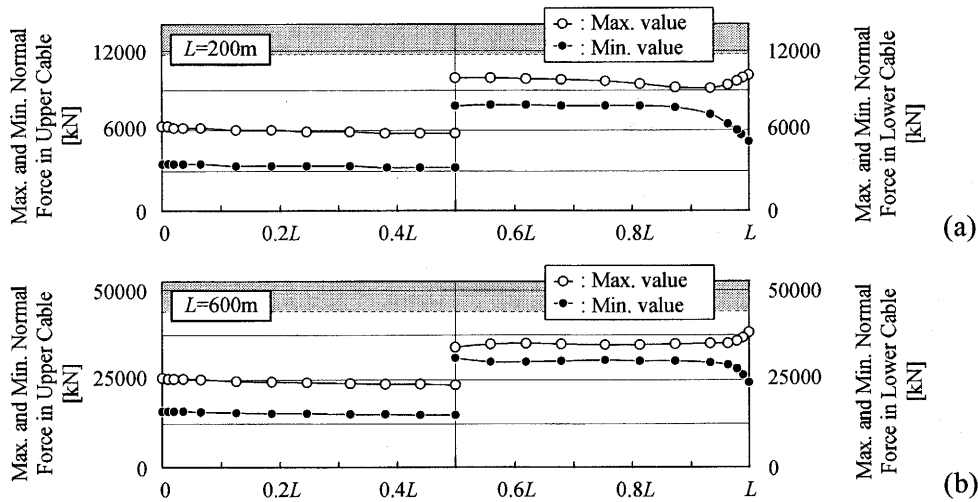


Fig. 11 The maximum and minimum normal force in the upper and lower cables for the bridges with $L=200\text{ m}$ ' and $'600\text{ m}$ ', (a) and (b).

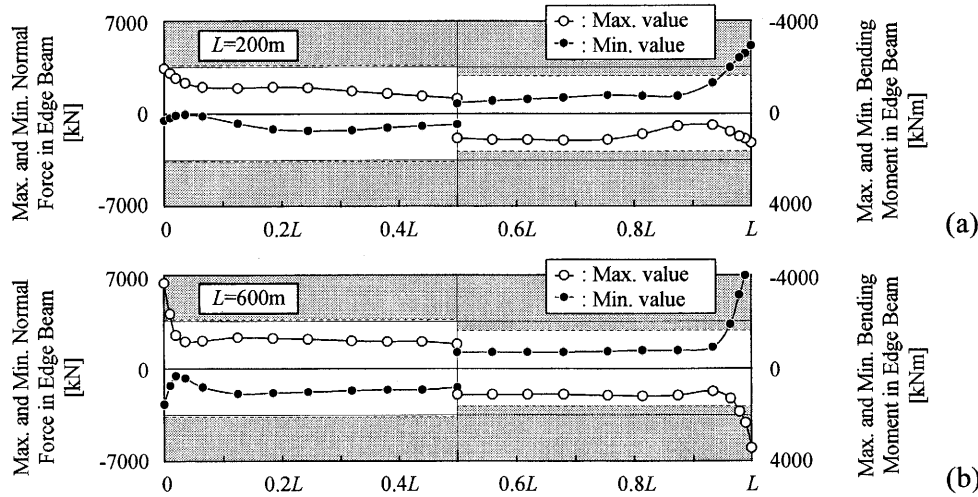


Fig. 12 The maximum and minimum normal force and bending moment in the edge beam for the bridges with $L=200\text{ m}$ ' and $'600\text{ m}$ ', (a) and (b).

difference also can be seen between these figures and Fig. 7 for the bridge with $L=400\text{ m}$.

Figs. 12(a) and (b) show the maximum and minimum normal force diagram together with the maximum and minimum bending moment diagram in the edge beam for the other two bridges with $L=200$ and 600 m , respectively. Qualitatively, a nominal difference also can be seen between these figures and Fig. 8 for the bridge with $L=400\text{ m}$.

Figs. 13(a) and (b) show the maximum and minimum extreme fiber stress diagram of combined bending moment and normal force in the edge beam for the other two bridges with $L=200$ and 600 m , respectively. In the structure with $L=200\text{ m}$, the maximum and minimum values are below the allowable stress of 140 MPa in the entire span. As regards the bridge with $L=600\text{ m}$, the maximum and minimum values were also far below the allowable stress in the

entire span except for the portion close to the abutment. This locally over-stressed problem also can be easily solved by partially using the welded circular pipe with higher strength steel with 255 MPa (SM570).

7. Feasibility of application of hybrid concept to vehicle bridges

The feasibility of the application of proposed hybrid stress-ribbon concept to vehicle bridges is discussed in this section. The important results of this study regarding the feasibility are itemized as follows:

The weight per unit deck area of the girder, which has two traffic lanes and one sidewalk, was estimated to be 3.5 kN/m^2 . This weight is only about half of the weight of a steel streamlined box girder for a conventional single span suspension bridge with two traffic lanes and one sidewalk.

For the proposed bridges with the span length of

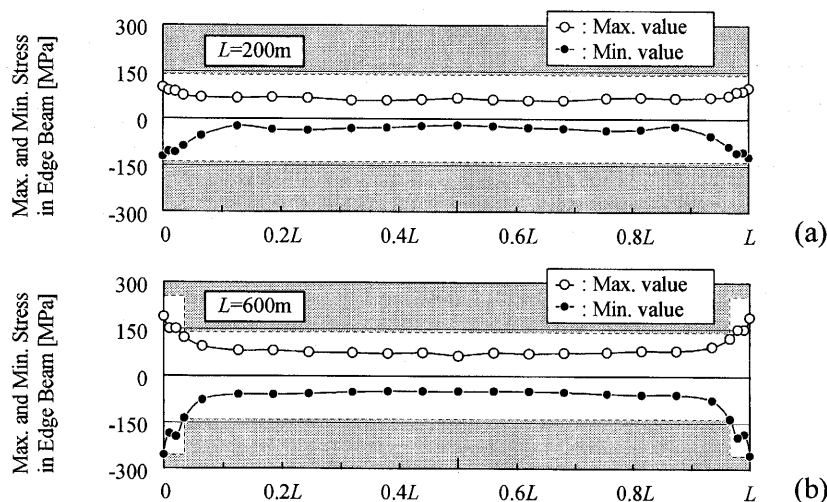


Fig. 13 The maximum and minimum extreme fiber stress due to combined normal force and bending moment for the bridges with $L = 200 \text{ m}$ and 600 m , (a) and (b).

200, 400 and 600 m, the total number of the upper and lower cable strand was respectively found to be 16, 40 and 60. The diameters of the 16-, 40- and 60-strand single cable were estimated to be 26, 40 and 50 cm and were not too large.

Regarding the static characteristics, the deformation and deflection of girder were well controlled by the upper cable, and the maximum normal force in the lower cable was 90% of the resisting force.

Although further studies should be made in order to realize the construction of the proposed bridges, which is the final objective of this study, the above results suggest that the design concept of the proposed hybrid stress-ribbon structure could be applied to vehicle bridges with a single span of 200-600 m.

8. Conclusions

The main results obtained in this study are summarized as follows:

1. The weight of the stiffening truss girder per unit area is about half of the weight of a streamlined steel box girder for a conventional suspension bridge.
2. For the bridges with the span length of 200, 400 and 600 m, the total number of the upper and lower cable strand was respectively found to be 16, 40 and 60. The diameters of the 16-, 40- and 60-strand single cable were estimated to be 26, 40 and 50 cm and are not too large.
3. The deformation of girder was well controlled by the upper cable.
4. The maximum girder deflection was 90% of the allowable value.
5. The maximum normal force in the lower cable was 90% of the resisting force. Also, compressive axial

force was not induced in the cables.

6. For the bridges with $L=400$ and 600 m , the maximum and minimum extreme fiber stress of combined bending moment and normal force in the edge beam are far below the allowable stress in the entire span except for the portion close to the abutment. This locally over-stressed problem can be solved by partially using higher strength steel.

The above results suggest that the design concept of the proposed hybrid stress-ribbon structure could be applied to vehicle bridges with a single span length of 200-600 m.

References

- 1) Tanaka, T. et al.: A Study on Improving the Design of Hybrid Stress-Ribbon Bridges and Their Aerodynamic Stability, *J. Wind Eng. and Industrial Aerodynamics*, Vol.90, pp.1995-2006, 2002.
- 2) Yoshimura, T. et al.: Static Characteristics and Aerodynamic Stability of Proposed Hybrid Stress-Ribbon Bridges, *Bull. Faculty of Eng., Kyushu Sangyo Univ.*, Vol.37, pp.237-244, 2000.
- 3) Yamada, S.: Seismic Response Characteristics of a Hybrid Stress-Ribbon Pedestrian Bridge, *Master's thesis, Kyushu Sangyo Univ.*, 2004.
- 4) Harada, T. et al.: Proposal for a Hybrid Stress-Ribbon Vehicle Bridge, *Proc. 3rd Int. Conf. on Advances in Structural Engineering and Mechanics*, pp.1111-1119, 2004.
- 5) Harada, T. et al.: Proposal for Hybrid Stress-Ribbon Vehicle Bridges – Part 2. Preliminary design of cables, *Bull. Faculty of Eng., Kyushu Sangyo Univ.*, Vol.43, to be published.